# Computational Fluid Dynamics of Air in Forced Draft Counter Flow Wet Cooling Tower: Using Comsol Multi-Physics.

**Abstract**

A cooling tower is a type of heat exchanger that uses air contact and water evaporation to chill water. The Port Harcourt refinery will be used as a case study in this paper's computational fluid dynamics CFD analysis of air flow in mechanical draft wet cooling towers**.** To achieve this, the CFD analysis of air under low Re-K-e flow conditions was done in Comsol Multi-Physics interface, The tower's schematic was created on AutoCAD. The results of the air's CFD analysis showed that the distribution profiles of velocity, temperature, relative humidity, and pressure inside the cooling tower are consistent with the air's postulated and calculated characteristics. AutoCAD was used to draw the schematic of the tower. The CFD analysis of air revealed that the velocity, temperature, relative humidity and pressure distribution profiles within the cooling tower are in accord with postulated and calculated characteristic of air within the Cooling Tower.

**Keywords: CFD Analysis, Counter Flow, Forced Draft, Wet Cooling Towers, Comsol Multi-Physics, PHRC.**



## 1. Introduction

According to Wikipedia, (2019) cooling Towers are mechanical devices that reject heat, this is made possible through the cooling tower setup's water evaporation in a stream of moving air. The combination of the rising airstream and the falling water causes the exit

air stream's temperature and humidity to rise. The cooled water is collected at the basin as the air is released to the surroundings via the evaporation of water in a moving air stream in the cooling Tower set-up. This interaction between the falling water and rising air streams leads to the increase in temperature and humidity of the exit air stream. While the air is discharge to the surrounding, the cooled water is collected at the basin. Wilbert and Jerold, (1982) posited that in most cooling towers serving refrigeration and air conditioning systems, one or more propeller or centrifugal fans are used to move air vertically up the Tower or horizontally via the tower. A large and significant surface area of water is provided by spraying the water through the sprinklers and down the tower from one baffle to another. CFD (computational fluid dynamics) models were created to simulate the functioning of cooling towers based on the mass/energy conservation laws and mass/heat transfer equations [Reuter and Kroger (2010), Klimanek, et al (2010)]. However, Smrekar, *et al.* (2011) held that the differences between the modelling world and the actual operations keep the simulation models from being utilized in the real-time operation. The precise goal is to simulate the airflow through a forced draft counterflow wet cooling tower using computational fluid dynamics. Comsol Multi-physics 5.4 is specifically applied in the computational fluid dynamics (CFD) of air as it flows through the Tower. To carry out a successful CFD analysis a good and simple diagram is priceless.

Chan, (2015), in his attempt to identify the formation of visible plume develop a concise mathematical model, Poppe Approach: it was used to carry out a validation test to identify the visible plume formation a cooling Tower in China. The validated CFD

simulation in combination with the water shedding approach, aided the conduct of CFD Simulation in an urban city environment. The CFD simulation results showed that there was a maximum reduction in temperature of 0.3[$^{o}$C] and maximum moisture content of 0.0003[-]

In this study, Heinrich (2010) used CFD to simulate the input losses of cooling towers, the effective flow diameter in the absence of a crosswind, and the pressure distribution around a cylinder subjected to a crosswind. Data from an experimental cooling tower configuration was utilized to evaluate the model. In order to enhance cooling tower inlet designs, the impact of various inlet geometries on the inlet loss coefficient and the effective diameter is examined. From result of the investigation it is found that using the k-ε realizable model, tetrahedral elements with an inlet diameter to cell size ratio of 700[-] and a turbulence intensity of between 2[%] and 10[ %] delivers the most accurate prediction of the inlet loss and effectiveness.

With the help of computational fluid dynamics, Rameshkumar et al. (2013) examined the distribution of temperature and air flow under various human loads inside the passenger compartment in steady-state settings. In the current inquiry, CFD analysis was used to simulate the temperature distribution and air flow in the passenger car cabin. It was found from the comparison's results that the predicted and experimental values are practically identical. It shown that the CFD model's forecast of the temperature and air flow distribution in a passenger car's cabin is accurate.

Vijayaragavan, *et al.* (2016), in this work used here ANSYS workbench for the CFD analysis of cooling tower. The boundary condition were set at; the inlet water

temperature 380[$^{o}$c], inlet air temperature 200[$^{o}$c], volume of circulating water circulated in cooling tower 30[$m^3$/hr]. CFD is used for performance and analysis of cooling tower because it helps in ascertaining terms of cooling efficiencies/effectiveness. When the water intake angle is reduced, so does the air inlet angle. As a result, cooling tower efficacy and efficiency rise. For the selected cooling Tower, the angle of 150[o] results in maximum efficiency and efficacy. Also, the air inlet angle increases with the increase in water outlet temperature, cooling efficiency and the reduction in effectiveness of the Cooling Tower.

The goal of Matilda's (2015) project was to use COMSOL Multi-physics to model a cooling tower system. As an experiment was being run on the setup, data was gathered. The model was fitted to the data in order to estimate the parameter; the parameter estimation was done using Matlab Live link, and Comsol Multi-Physics was used for the simulation. In order to calculate the heat transport coefficient, Onda's approach is utilized to estimate the value of the parameter, h. The heat transmission coefficient varies between 14.5 and 15.7 [kW/m2°C] because the term h is expected to be 30.6 [kW/m2°C].

## 2. Materials and Method

### 2.0 Description of Study Area

According to the Department of Petroleum Resources report (2014), the Port Harcourt Refining Company, (PHRC), is an indigenous oil and gas company domicile in Nigeria whose core mandate is primarily the refining of crude oil into petroleum products. The company is situated in Eleme Elesa area of Rivers State, South-South Nigeria. The company is a subsidiary of the Nigerian National Petroleum Corporation (NNPC).

Nwachukwu, (2010), It is regarded as the biggest oil refining company in Nigeria with the company operates two oil refineries with a combine capacity of capacity of 210,000 barrels per day. The cell is made up of the component listed as follows: a draft fan, baffles, drift eliminators, collecting basin, open air inlets windows, water sprinklers, pumps etc. It is a forced draft wet Cooling Tower.

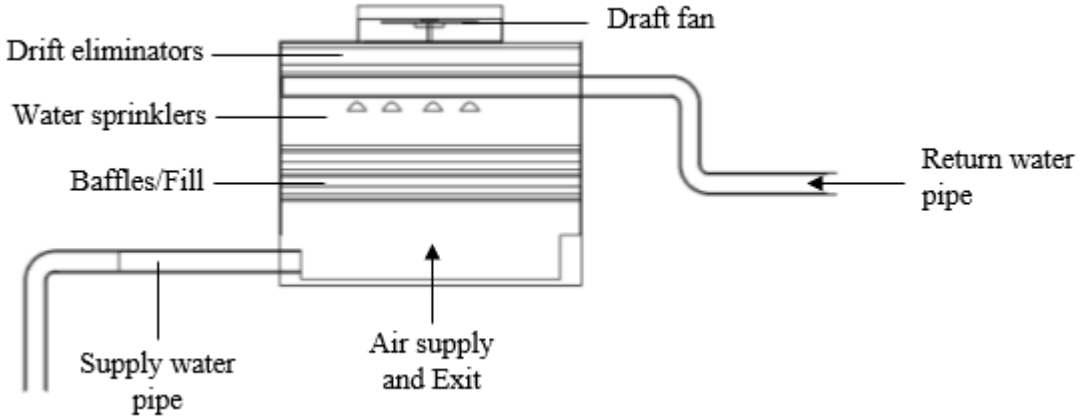


Fig 1. Cell unit of PHRC Cooling Tower

Fans: it functions to forced significant amount of air across the tower in an effective manner These fans are driven by An electric motor assembly; Drift Eliminators: These help in capturing water droplets entrapped in the air stream at the exit point to the surrounding; Fills/Baffles: They act to convert the water into droplets by breaking its momentum; also, it helps improve efficiency by expanding the surface area of water and in the process improve the interaction time between air and the water; Water Basin: It serves as a reservoir water for that flows down through the tower and fills

## 2.1 Model description

## 2.2 Model Building in Comsol Multi-Physics

The model was built in a CFD software, Comsol multi-physics which allows the combination of different physics in simulation. The physics used in the present study includes, fluid flow, heat transfer and moisture transport. The airflow is modeled under the Turbulent Flow, Low Re k-ε interface conditions because the Reynolds number is about 1500. With the Low Re k- ε turbulence model, the turbulence variables are solved in the whole domain down to the walls and thus provide accurate input values for the transport equations. Note that because the mass contribution due to the evaporation is small at the water surface, a wall (no slip) condition is used on this boundary for the airflow computation. The Eulerian-Eulerian model enables the building of local mass and momentum equations for each phase as well as the corresponding interfacial contact conditions. Equation conservation of energy, momentum, and mass corresponds to the main and overriding equations; thus, the Low Re k-ε Equations equations for the momentum balance of the water phase and air phase it is represented by the following expression,

$$\rho(u.\nabla)u = \nabla.[-pl + K] + F \quad (1)$$

$$\rho\nabla.(\nabla) = 0 \quad (2)$$

$$K = ((\mu + \mu_T)(\nabla u + (\nabla u)^T) \quad (3)$$

$$\rho(u.\nabla)k = \nabla.\left[\left(\mu + \frac{\mu_T}{\sigma_k}\right)\nabla_k\right] + P_k - \rho\epsilon \quad (4)$$

$$\rho(u.\nabla)\epsilon = \nabla.\left[\left(\mu + \frac{\mu_T}{\sigma_k}\right)\nabla_\epsilon\right] + C_{\epsilon 1}\frac{\epsilon}{k}P_k - C_{\epsilon 2}\rho\frac{\epsilon^2}{k}f_\epsilon(\rho\mu k\epsilon J_w), \in = ep \quad (5)$$

$$\nabla G.\nabla G + \sigma_w G(\nabla.\nabla G) = (1 + \sigma_w)G^4, \;\; l = \frac{1}{G} - \frac{l_{ref}}{2} \quad (6)$$

$$\mu_T = \rho C_\mu \frac{k^2}{\epsilon} f\,\mu(\rho\mu k\epsilon l_w \quad (7)$$

$$P_K = \mu_T[\nabla u : (\nabla u + (\nabla u)^T] \quad (8)$$

Also, the Heat Transfer in Moist Air and the Moisture Transport in Air equations are represented by equation (9 to 10) and equations (11 to 13) respectively.

$$\rho c_p u.\nabla_T + \nabla.\mathrm{q} = \mathrm{Q} \quad (9)$$

$$\mathrm{q} = -\mathrm{k}\nabla_T \quad (10)$$

$$M_v u.\nabla_{C_v} + \nabla.\mathrm{g} \quad (11)$$

$$\boldsymbol{g} = M_v D.\nabla_{C_v} \quad (12)$$

$$c_v = \phi c_{sat} \quad (13)$$



## 3. CFD Simulation Procedure

### 3.1 Modeled Cooling Tower Description

In Comsol multi-physics 5.4, the geometrical characteristics of the modeled cooling tower in Fig 2 is described as consisting of a space dimension of 3 with 29 domains, 294 boundaries, 624 edges and 372 vertices).

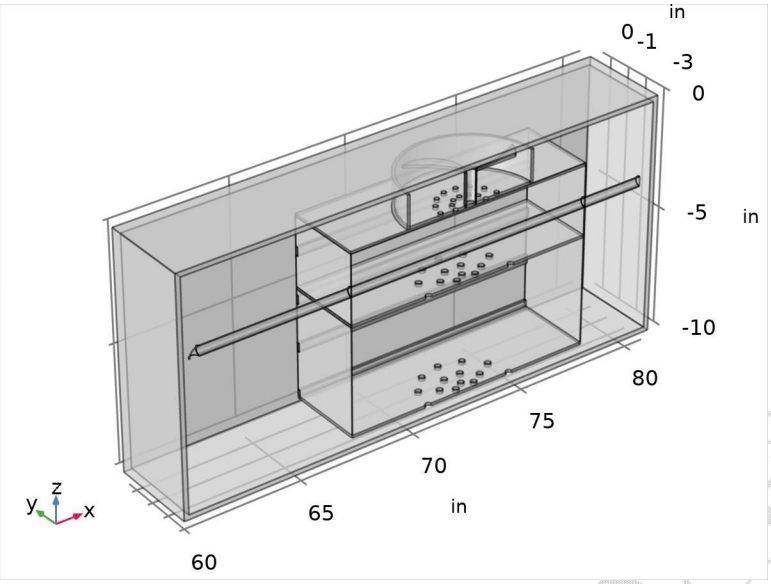

Fig 2 Modeled Geometry of the cooling tower



### 3.1.1 Boundary condition

**Table 1: Initial values for Key simulation parameters**

| Parameters | Velocity [m/s] | Pressure [Pa] | Temperature [K] | Relative humidity [-] | Evapouration Rate |
|---|---|---|---|---|---|
| Values | 0 | 0.03 | 293.15 | 0.0189 | 1.725 |

The initial values applied at the beginning of the simulation are staed in Table 1

### 3.2 Material Selection

The following figures shows the material selection of the different component of the cooling Tower during simulation in Comsol multi-physics. The properties of the different materials used in the simulation as shown in tables in Table 2, Table 3 and Table 4 were in-built.

**Table 2: Properties of concrete selected for the cooling tower geometry**

| Property | Value |
|---|---|
| Coefficient of thermal expansion | {{10e-6[1/K], 0, 0}, {0, 10e-6[1/K], 0}, {0, 0, 10e-6[1/K]}} |
| Density | 2300[kg/m^3] |
| Thermal conductivity | {{1.8[W/(m*K)], 0, 0}, {0, 1.8[W/(m*K)], 0}, {0, 0, 1.8[W/(m*K)]}} |
| Heat capacity at constant pressure | 880[J/(kg*K)] |
| Young's modulus | 25e9[Pa] |
| Poisson's ratio | 0.20 |

**Table 3: Properties of PVC selected for the cooling tower geometry**

| Description | Value |
|---|---|
| Coefficient of thermal expansion | {{100e-6[1/K], 0, 0}, {0, 100e-6[1/K], 0}, {0, 0, 100e-6[1/K]}} |
| Relative permittivity | {{2.9, 0, 0}, {0, 2.9, 0}, {0, 0, 2.9}} |
| Density | 1760[kg/m^3] |
| Thermal conductivity | {{0.1[W/(m*K)], 0, 0}, {0, 0.1[W/(m*K)], 0}, {0, 0, 0.1[W/(m*K)]}} |
| Young's modulus | 2.9e9[Pa] |

**Table 4: Properties of low carbon steel selected for the cooling tower geometry**

| Description | Value |
|---|---|
| Electrical conductivity | {{8.41[MS/m], 0, 0}, {0, 8.41[MS/m], 0}, {0, 0, 8.41[MS/m]}} |
| Relative permittivity | {{1[1], 0, 0}, {0, 1[1], 0}, {0, 0, 1[1]}} |

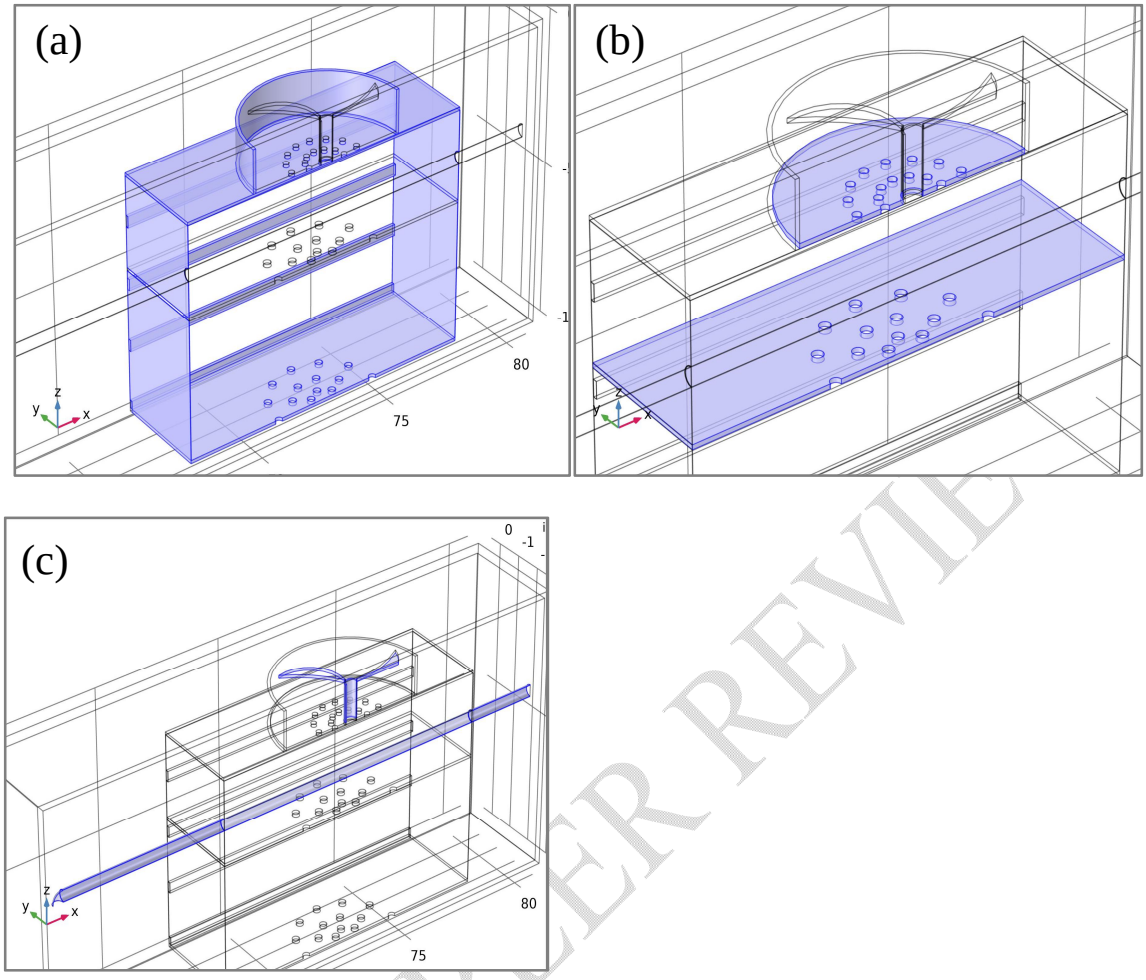


Fig 3 Categorization and selection of Materials

**(a)** concrete section of the cooling tower geometry **(b)** Polyvinyl chloride. (Domains 3, 5, 8, 15–19 were selected as concrete following the design characteristics while domains 13, 20 for PVC)). **(c)** Low Carbon Steel 1002, (Boundaries 11, 13–14, 16, 72, 75, 112–113, 160–161, 163, 167, 194, 207–208, 287, 289).



Fig 3 highlights the materials used for the different segments and domain of the cooling tower. The highlighted domain of Fig 3(a) depicts the concrete component of the cooling tower, Fig 3(b) highlighted parts represent the baffles and drift eliminator whose material constituent is Polyvinyl chloride, also the highlighted section of Fig 3(c) which are fan blade and water supply pipe are both made up of steel.

### 3.3.1 Plots of Water and Air properties

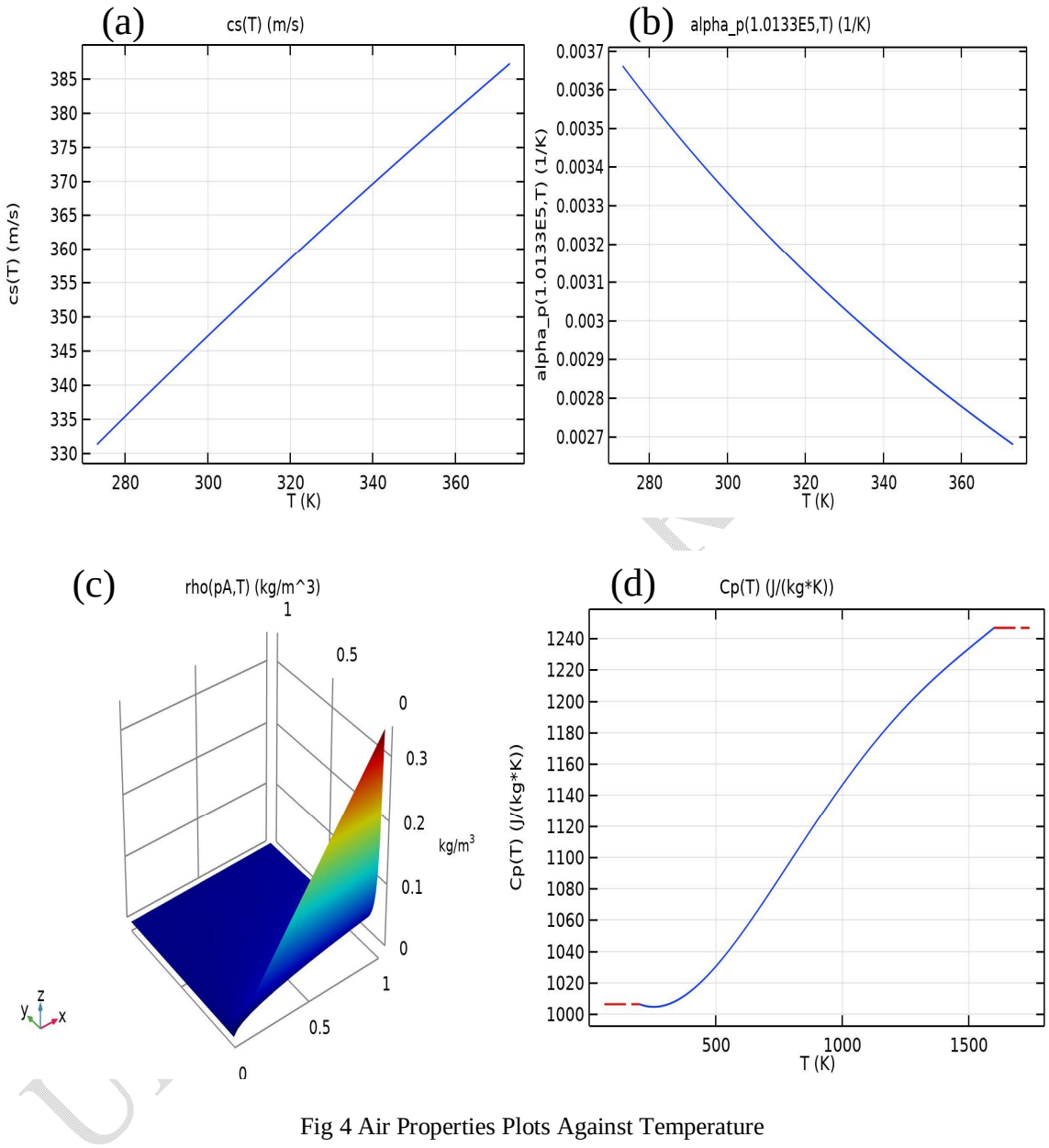


Fig 4 Air Properties Plots Against Temperature

(a)Speed of Sound(cs) Vs Temperature; (b) Coefficient of Expansion vs Temperature; (c) Density Vs Temperature; (d) Specific Heat Capacity Vs Temperature

The comsol plots of Fig 4 clearly shows the interaction among the material properties of air. Sound speed and specific capacity of air increases with temperature while the coefficient of expansion decreases with air temperature.

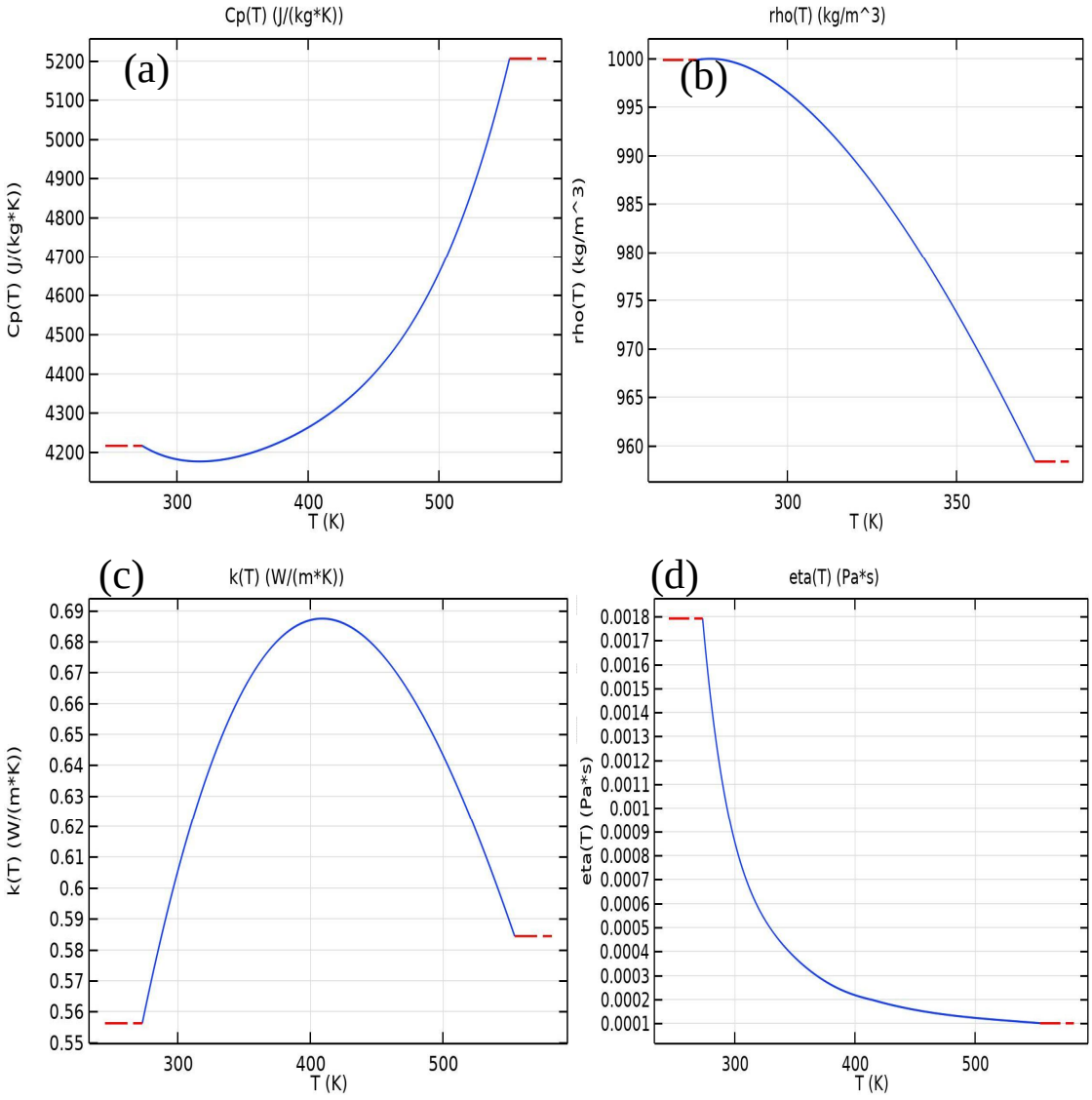


Fig 5 Water Properties Plots Against Temperature

(a) Specific Heat Capacity Vs Temperature; (b) Coefficient of Expansion vs Temperature; (c) Thermal conductivity Vs Temperature; (d) Dynamic viscosity Vs Temperature

The comsol plots of Fig 5 clearly shows the interaction among the material properties of water. The density and dynamic viscosity of water increases with the temperature, specific capacity increases with temperature, while thermal conductance produces a concave quadratic curve with temperature.

### 3.3.2 Domain Segmentation and Description

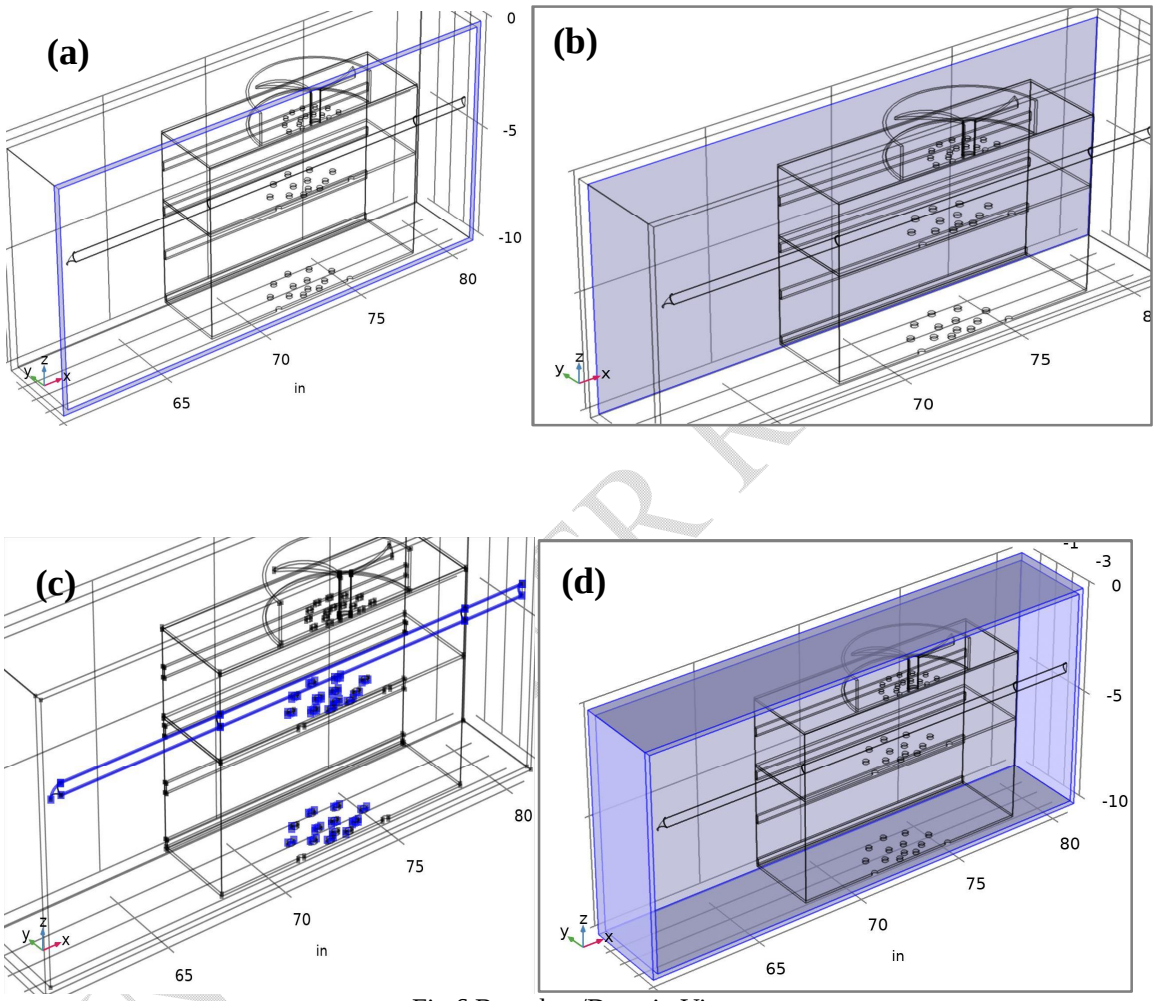


Fig 6 Boundary/Domain Views

**(a)** The wall **(b)** Air inlet of the cooling tower (selection, 9 boundaries) **(c)** Water Flow Path(in Blue) **(d)** Air Domain Symmetry (Boundaries 1, 3–8, 293–294)

The selected edges for water flow in Fig 6 (c) are **(***20, 28, 33, 113, 117, 155, 179–180, 192, 213–214, 219, 222–223, 232, 259, 264, 267, 269, 271, 275, 320–321, 327, 337, 346, 417–418, 425–426, 440, 442, 472, 477, 479, 482, 485, 490, 508–509, 516, 605, 609, 615)* while that of air flow boundaries in Fig 6 (d) is within these boundaries *(1, 3–8, 293–294)*

### 3.3.3 Generated Mesh

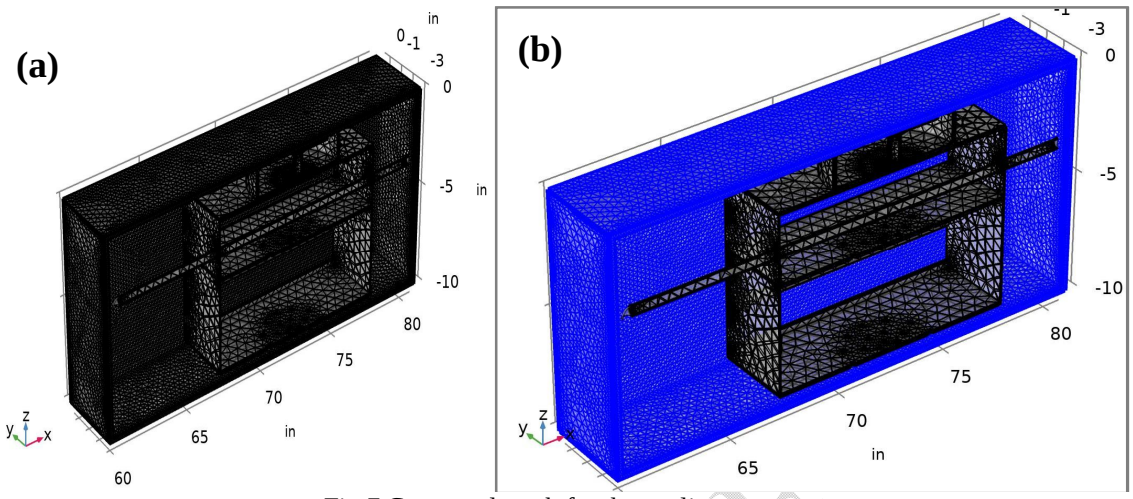


Fig 7 Generated mesh for the cooling tower
**(a)** the cooling tower mesh **(b)** control volume mesh

Average element quality (0.1112), tetrahedron (102487), pyramid (6160), prism (330212), triangle (54152), edge element (4558) and vertex element (366) for the control volume mesh. While the cooling tower mesh has maximum element size (0.618), minimum element size (0.185) with curvature factor of 0.7, resolution of narrow regions (0.6), maximum element growth rate (1.2) and the predefined size is coarse. The mesh was calibrated for fluid dynamics.



## 4. Results and Discussions

This section presents the output of the simulation results of the air fluid analysis (CFD) as modeled in Comsol Multi-Physics 5.4.

One of the biggest and most often used heat and mass transfer systems, the cooling tower, was examined using the CFD approach in this dissertation.. An explicit model of cooling towers was employ to analyse air as it flows through the Cooling Tower (see fig 2). The process of altering the air and water temperatures as well as the driving potential for convection and evaporation heat transfer as it changes the tower's height clearly demonstrates the cooling towers' thermal performance (see fig. 8). (a to d). Inside the cooling tower, the evaporation heat transfer rate is substantially higher than the convective heat transfer rate (Zubair et al., 2003). The total heat transfer rate in the cooling tower is greatly influenced by each kind of heat transfer rate.

Convection, conduction, and evaporation all contribute to the gradual cooling of the water over time. As air flows away from the water's surface, its relative humidity value decreases from 100 to 20 [percent] accordingly. Air can absorb more water because of the high temperature. Evaporation in this model is responsible for a drop in temperature of roughly 10 [K] at the conclusion of the simulation.



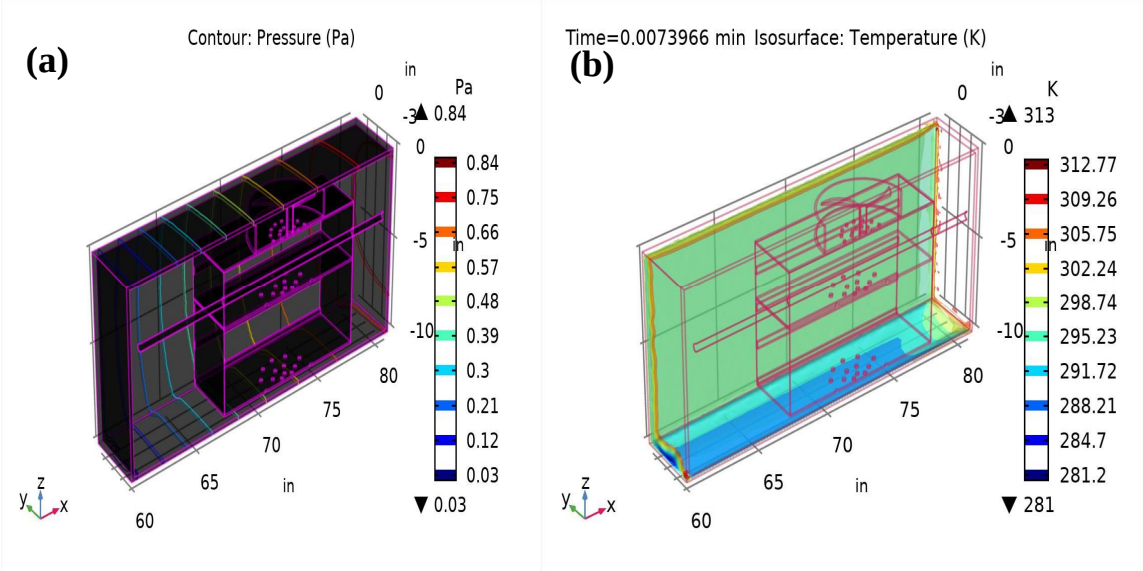

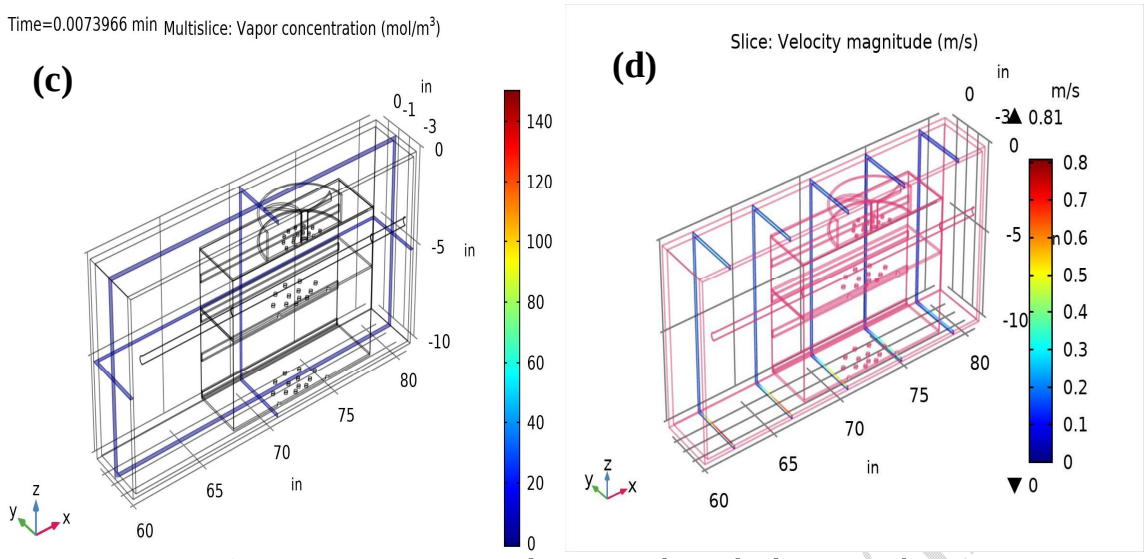


Fig 8 Pressure, Temperature, Relative Humidity and velocity Distribution
**(a)** Pressure Profile; **(b)** temperature Profile; **(c)** Relative humidity Profile; (d) Velocity Profile

The discussion will be further broken down into the following;

### i. Velocity Distribution

Fig 8(d), it is clearly seen from the modelling values that the velociy of air increases as it moves from the entry point at the base of the Tower towards the exit points where the draft fan is located. The value increase from 0m/s to about 0.8m/s. This value falls within the computed range of values for the refiniries under consideration.

These profiles demonstrate how the air suffers a velocity decrease as it passes through the tower devices due to the no-slip condition over the wall of internal devices, with the maximum velocities occurring at the fan intake.At the packing area is where major loss of momentum happens, due to the close spacing between the different lamellas in zigzag from the packing. Also, the lamellas increase the air pressure drop. The drift eliminator area is short, which causes a velocity loss. From the analysis of the velocity profiles, it was initially determined using the R-e turbulence model.

### ii. Pressure Distribution

The values of air pressure from the CFD analysis as stated in Fig 8 (a) ranges from 0.033[bar] to 0.84[bar]; the values also falls within the range of the month on month calculated vales of the case study with vales between 0.028[Bar] to 0.05[bar]. As the air passes through the cooling Tower towards the exit, it picks more and more molecules of water and subsequently the pressures of the air molecule increases just as our modelled capture it. In addition, there is a pressure gain as the air goes through the packing and drift eliminator, due to the no slip boundary condition in the internal parts of the cooling tower. This increase even though it fluctuates as it encounters the packing unit, it eventually increases as it approaches the draft fan around the exit.

### iii. Relative Humidity Distribution

Also, From fig 8 (c), the model show that the relative humidity of the air increases as the air flows throught the Tower, it picks up more water molecule and as a result the number the volume of water vapour in the increases considerably.The model results agrees with the calculated and measured results from the study. The relative humidity increases range as dipicted by the Tower is between 0 to 100[%]. Further more, the transport mechanism of energy in this area is given by forced convection due to the velocity differences in the boundary layer of the phases. As seen from the profile the temperature increases reasonably as the air interacts with the water. Both mass transfer and heat transfer takes.

### iv. Temperature Distribution

Figure 8(b) illustrates the rise in air temperature as it ascends the tower, through the packing section, and through the drift eliminator portion. The highest temperatures shown were for the temperature of the air exit, which is 312.77[K].

## 5 Conclusion

i. There is a pressure gain as the air goes through the packing and drift eliminator, due to the no slip boundary condition in the internal parts of the cooling tower. This increase even though it fluctuates as it encounters the packing unit, it eventually increases as it approaches the draft fan around the exit. As the air passes through the cooling Tower towards the exit, it picks more and more molecules of water and subsequently the pressures of the air molecule increases just as our modelled capture it.

ii. The relative humidity of the air increases as the air flows throught the Tower, it picks up more water molecule and as a result the number the volume of water vapour in the increases considerably.The model results agrees with the calculated and measured results from the study.

iii. The transport mechanism of energy in this area is given by forced convection due to the velocity differences in the boundary layer of the phases.

v. As seen from the profile the temperature increases reasonably as the air interacts with the water.



**Notations**

Cp Specific heat capacity at constant pressure (KJ/kgK)

Cv Saturation vapour concentrstion

$G_k$ Generation of turbulent kinetic energy due to mean velocity gradients

$G_b$ Generation of turbulent kinetic energy due to buoyancy k Turbulent kinetic energy/($m^2 s^{-2}$)

u fluid velocity,

p fluid pressure,

ρ fluid density, and

F external forces applied to the fluid

K Kinetic Energy

P pressure

**Greek symbols**

P Density of air at inlet to the filter housing/(kgm–3 )

γ Uniform index

μ Dynamic viscosity/(Pas)

σε Turbulent Prandtl number

ε Turbulent energy dissipation rate/($m^2 s^{-3}$)

$\mu_T$ Turbulent viscosity

k Turbulent kinetic energy

ϵ turbulent dissipation

**References**


Arora, C.P (2006). Refrigeration and air–conditioning. Tata McGraw-Hill Publishing Company Limited,New Delhi. ISBN 0-07-463010-5

ASHRAE Handbook, (2008). HVAC Systems and Equipment (SI), *American Society of Heating, Refrigeration and Air Conditioning Engineers, Inc.. ASHRAE*

Bowman, C. F. (1995). Cooling Tower Performance Presented at *The Epri Thermal Performance Improvement Seminar*. Available at: https://www. researchgate.net/ pub lication/265550423

Chan, J. K and Golay, M. W. (*1977*) Comparative Evaluation of Cooling Tower Drift Eliminator Performance. *energy laboratory report no. mit-el 77-004.*

Cooling Tower Institute. (1990) CTI Code Tower. Standard specifications, acceptance cooling tower operation. Energy Convers Manage 2009;50(9):2200–9.

Cortinovis GF, Paiva JL, Song TW, Pinto JM. (2009) A systemic approach for optimal draft cooling tower. *Numer Heat Transfer A-Appl;57(2):119–37.* Eng & Tech. Journal, Vol29, No.6, 2011

Donald K and Michael R. (2007). Assessing the Performance of Cooling Towers and Their Effect on Chiller Efficiency. *Center for Advanced Energy Systems*

Hayder, H. M. (2012). An Energy and Exergy Analysis on the Performance of Wet Cooling Tower in Iraq. *Republic of Iraq Ministry of Higher Education and Scientific Research Al-Mustansiriyah University College of Engineering Mechanical Engineering Department*

Heidarinejada, G, Karamia, M., Delfanib, S. (2009). Numerical simulation of counter-flow wet-cooling towers. *International journal of refrigeration*

Him, C. M. (2015). Cooling Tower Performance Analysis and Visible Air Plume Abatement in Buildings Situated in Temperate Climate Zone. *A thesis submitted to the Welsh School of Architecture, Cardiff University*

Kariem, N. O.and Jaffal* H. M. Performance of Cooling Tower with Honeycomb Packing. *College of Engineering, University of Al-Mustansiriya / Baghdad*

Kashania, M. M. and Dobregob, K. V. (2013). Heat and Mass Transfer In The Over-Shower Zone Of A Cooling Tower With Flow Rotation *Journal of Engineering Physics and Thermophysics,* Vol. 86, No.6,

Khan JR, Qureshi BA, Zubair SM. (2004). A comprehensive design and performance evaluation study of counter flow wet cooling towers. *Int J Refrig;27(8):914–23*

Klimanek A, Bialecki RA, Ostrowski Z. (2010) CFD two-scale model of a wet natural draft cooling tower. *Numer Heat Transfer A-Appl;57(2):119–37.*

Satish, K. (2016). Performance Analysis of Cooling Tower. *International Journal of Engineering Trends and Technology (IJETT) – Volume 38 Number9* ISSN: 2231-5381.Available online at: http://www.ijettjournal.org

Matilda Lundberg (2015). Modeling & Simulation of a Cooling Tower with COMSOL Multiphysics. *Department of Chemical Engineering Lund University*

"Multiphysics Simulation Software - Platform for Physics-Based Modeling." [Online]. Available: http://www.comsol.com/comsol-multiphysics. [Accessed: 07-Febrauary-2019].

Pan TH, Shieh SS, Jang SS, Tseng WH, Wu CW, Ou JJ. (2011). Statistical multi-model approach for performance assessment of cooling tower. *Energy Convers Manage 2011;52(2):1377–85.*

Pranav Yedatore Venkatesh, P. Y. (2015). Creating a New Model to Predict Cooling. Tower Performance and Determining Energy Saving Opportunities through Economizer Operation. *ScholarWorks@UMass Amherst*

Qureshi, B. and Zubair, S. (2007) Second-Low Based Performance Evaluation of Cooling Towers and Evaporative Heat Exchangers, *International Journal of Thermal Sciences, Vol.46, pp (188-198)*.

Rameshkumar.A1, Jayabal.S, and Thirumal.P (2013). CFD Analysis of Air Flow And Temperature Distribution In An Air Conditioned Car. *Temperature Distribution in an Air Conditioned Car Article. Avaialble Online at: https: //www.res earchgate.net/ pu b liccation/268517199.*

Rajput, R. (2008). Refrigeration and air–conditioning. *S.K Kataria and Sons; Darya Ganj,New Delhi-110002*

Reuter HCR, Kroger DG. (2010). A new two-dimensional CFD model to predict performance of natural draught wet-cooling towers packed with trickle or splash fills. *Proc ASME Int Heat Transfer Conf ;4:589–98.*

Oko, C and Ogoloma, (2011) Generation of Typical Meteologic All Year Round for Port Harcourt Zone. *Journal of engineering technology vol 6, Nun 2, 2011,pp.204-214*

Smrekar J, Kustrin I, Oman J. (2012) Methodology for evaluation of cooling tower performance – Part 1: description of the methodology. *Energy Convers Manage ;52(11):3257–64.*

Smrekar J, Senegacnik A, (2012). Fuhrer C. Methodology for Evaluation of Cooling Tower Performance – Part 2: Application of the Methodology and Computational aspects of Poppe Equations. *Energy Convers Manage ;52(11):3282–9.*

Smrekar, J., Kuštrin I., Omanb, J. (2011). Methodology for Evaluation of Cooling Tower Performance. *Energy Conversion and Management 52 (2011) 3257–3264.*Available at: –www.elsevier.com/locate/enconman1

Smrekar, J., Oman, J., S˘irok., B. (2005) Improving the efficiency of natural draft cooling towers. *Energy Conversion and Management*. Available online www . elsevier .com/locate/enconman

Söylemez, MS. (2004). On the optimum performance of forced draft counter flow Cooling towers. *Energy Convers Manage;45(15/16):2335–41*.

Störm. H. C. (2010) CFD investigation of flow in and around a test for water-cooling towers, Part I, Part II and Part III, CTI Code ATC-105, revised.

Ubabuike, U. H. (2012) Design of an Efficient Cooling Tower for Alaoji Power Plant, Aba, Abia State, Nigeria. *IOSR Journal of Engineering Apr. 2012, Vol. 2(4) pp: 731-737 ISSN: 2250-3021.*Available online at: www.iosrjen.org pg 731

Vijayaragavan1, A. Arunraj, S. Parthasarthy, P. Raj, S. P Ali, A. A. (2016). Performance and Analysis of Cooling Tower. *International Research Journal of Engineering and Technology (IRJET) e-ISSN: 2395 -0056 Volume: 03 Issue: 04. Available online at:* www.irjet.net p-ISSN: 2395-0072

Wang, Q., Wang, P., S. U, Z. (2008). An Analytical Model on Thermal Performance Evaluation of Counter Flow Wet Cooling Tower. *Key Laboratory of Energy Thermal Conversion and Control, Ministry of Education, School of Energy and Environment, Southeast University.*

Wilbert, F.S and Jerold, W.J (1982). Refrigeration and air conditioning. *McGrwa-Hill Co Books International Singapore*.

Xiaoni Qi, Yongqi Liu and Zhenyan Liu, (2013) "Exergy Based PerformanceAnalysis of a Shower Cooling Tower*", Journal of Mechanical Engineering, Vol.59, No.4, pp (251-259)*.

Yao Y, Lian ZW, Hou ZJ, Zhou XJ. (2004). Optimal operation of a large cooling system based on an empirical model. *Appl Therm Eng;24(16):2303–21*.

Zubair, S. M., Yaqub, M. and Jameel-Ur-Rehman, K. (2003). Performance characteristics of counter flow wet cooling towers. *Energy Conversion and Management 44 (2003) 2073–2091. doi:10.1016/S0196-8904(02)00231-5.*